ISSN: 2521-0904 (Print)
ISSN: 2521-0440 (Online)

Engineering Heritage Journal / Galeri Warisan Kejuruteraan 1(1) (2017) 29-35

Contents List available at RAZI Publishing

Engineering Heritage Journal / Galeri Warisan Kejuruteraan

Journal Homepage: http://www.razipublishing.com/journals/galeri-warisan-kejuruteraan-gwk/

https://doi.org/10.26480/gwk.01.2017.29.35

The Efficiency of Structural Steel Section with Perforated-Corrugated Web Profile Subjected to Shear Loading Condition

Fatimah De'nan[1*], Hazwani Hasan[2,b], Choong Kok Keong[3,c]

[1,2,3] School of Civil Engineering, Universiti Sains Malaysia, 14300 Nibong Tebal Penang, Malaysia.
*cefatimah@usm.my, [b]wawani127@yahoo.com, [c]cekkc@usm.my

ARTICLE DETAILS

Article history:
Received 16 September 2016
Accepted 27 December 2016
Available online 10 January 2017

Keywords:
Perforated web profile, corrugated web profile, finite element analysis, efficiency, shear buckling capacity

ABSTRACT

Triangular web profile (TriWP) steel section with various combinations of perforation shapes, sizes and layouts of perforation are investigated under shear loading condition. The aim of this study is to determine the structural efficiency based on the ratio of buckling load, P_b to the self-weight of the model. For this purpose, the specimen with three different perforation size between 0.4D to 0.6D, five perforation shapes i.e. circle, square, hexagon, diamond and octagon and three different layouts of perforation, which are Layout 1, Layout 2 and Layout 3 are analyzed by using LUSAS software. It involves two stages of analysis which are Stage 1 and Stage 2. In Stage 1, the most efficient perforation shape, size and layout of perforation is determined based on the highest structural efficiency value. From the result obtained, the TriWP with perforation of diamond in shape and 0.4D in size arranged in Layout 3 shows the highest structural efficiency value i.e. 204.75 produced from the highest buckling load. It shows the lowest percentage difference of efficiency compared to that of TriWP without perforation i.e. 16.39%. It leads to the most efficient perforation shape, size and layout. Then this type of model is analyzed for different section properties and span length to observe the effect performance and its structural behavior under Stage 2. It observed that, shear buckling capacity increase proportional to the web thickness. Meanwhile, when the span length is increase from1 m to 5 m, the shear buckling capacity reduce.

1. Introduction

The growing popularity of perforated steel plates since 1940's is due to cost efficiency, ease of fabrication, high strength to weight ratio and suitability for a wide range application [2]. In order to provide better understanding of stress distribution in the vicinity of the web openings, some researches try to examine numerically the web opening shapes of perforated steel sections and identify those that have the best structural behaviour under certain type of loading. [2,3] The aim is to provide the maximum possible web opening area for the integration of services, whilst keeping the minimum possible self-weight for different type of loading.

In order to provide data for the development of a design model for the shear capacity of steel girders with web openings, with and without transverse stiffeners and opening reinforcements, a numerical simulation was performed by Hagen et al. (2009) in designing the girder in a state of pure shear at the opening center. Based on the numerical data, a design model is presented that accounts for the reduction in webs shear area, shear buckling of the web and the effect of opening position, vertical stiffeners and opening reinforcement.

Darehshouri et al. (2013) reported that the results obtained for circular, square and rectangular openings shows that the ultimate shear capacity was influenced significantly with size of opening, nearly 30% drop of shear capacity when the depth of openings was increased to half the web depth of girders. Meanwhile, Hamoodi (2013) found that the presence of openings in the web section of plate girder had reduced the ultimate shear load about 51%. Shear strength were considerably reduced by the presence of web opening [8] and its decrease with increase the perforation sizes [17].

On the other hand, introduce the corrugated steel web solely provides the shear capacity of the girders where the shear strength is controlled by buckling and/or steel yielding. Eldib (2009) performed finite element analysis to study the geometric parameters affecting the shear buckling strength of curved corrugated steel webs for bridges. The curved corrugated webs produce a tremendous increase in shear buckling strength and considerable weight saving in regard to the corresponding trapezoidal corrugated webs. The corrugation angle has a considerable effect on the behaviour of curved corrugated webs, where higher corrugation angles produce a tremendous increase in the shear buckling strength.

In case of trapezoidally corrugated steel web, a few researchers such as Moon et al. (2009), Yi et al. (2008) and Nie et al. (2013) had studied the shear strength and design of this corrugated steel web. Trapezoidally corrugated steel plates have been used as the web of pre-stressed concrete box-girder bridges to reduce dead load and increase structural efficiency. Due to an applied shear stress, the trapezoidally corrugated web can fail by three different shear buckling modes: local, global, and interactive shear buckling as shown in Fig. 1. Local buckling involves a single panel, whereas global buckling involves multiple panels, with buckles extending over the entire depth of the web.

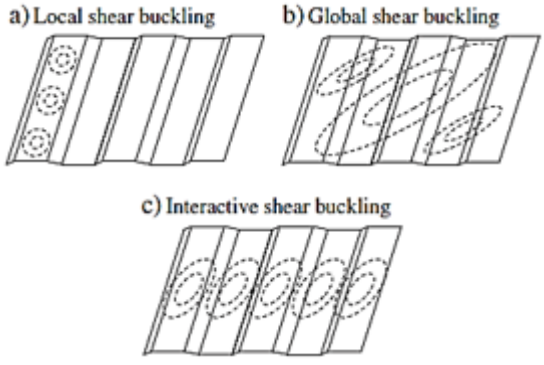

Fig. 1 Three different shear buckling modes of trapezoidal corrugated steel webs [14]

Since the trapezoidally corrugated web profile was replaced by Triangular Web Profile (TriWP) in enhanced the shear buckling strength, Triangular Web Profile (TriWP) steel beam was modelled by De'nan and Hashim (2012) as an innovation in steel design. However, in terms of weight, TriWP tends to have greater weight than the flat web because of the corrugation profile. Thus, to improve the usage of the steel beam in the building construction, perforation shapes such as circular, square, hexagonal, octagonal and diamond are proposed in this research.

The idea of perforated-corrugated web profile in achieving efficient structural steel section can reduce the weight of the steel section and may achieve similar performance to those without opening. Furthermore, the structural capacity of TriWP with perforation not yet studied. Hence, the determination of the structural efficiency of TriWP with the combinations of different perforations shapes, sizes and layouts are needed. A three-dimensional finite element model using LUSAS is performed to analyse the structural efficiency and structural behaviour of TriWP with perforation subjected to shear loading. In addition, the effect of section properties and span length on the structural behaviour and performance of TriWP with perforation need to be observed.**2. Model Description**

In this research, the TriWP with perforation is analysed. The model with section properties of 200 mm web depth; 100 mm flange width; 6 mm flange thickness and 4 mm web thickness with 900 mm span length which is used to carry out the study. As illustrated in Fig. 2, TriWP with perforated web consists of two flanges welded to the triangular profile of the perforated web section.

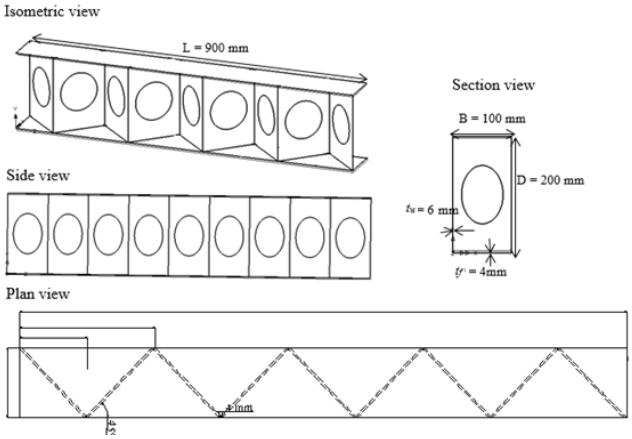

Fig. 2 Profile of TriWP with perforation

2.1 Perforation Shapes and Sizes

Perforations in the shape of circle, square, hexagon, diamond and octagon are proposed in this research as shown in Fig. 3. The perforations with the sizes of 0.4D, 0.5D and 0.6D (80 mm, 100 mm, 120 mm) where D is the depth of the section are generated. The perforation shapes as the function of perforation of the web section allows piping system and ducting services to pass through.

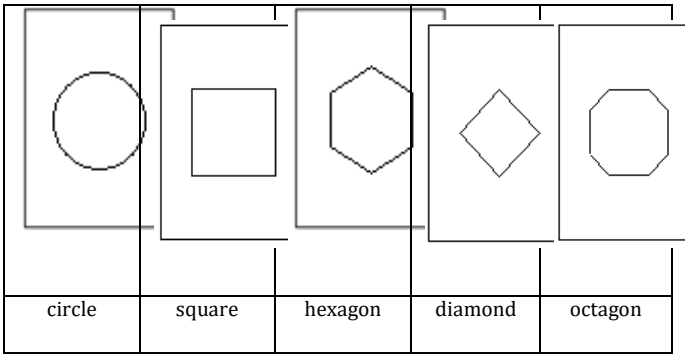

Fig. 3 TriWP with perforation

2.2 Layouts of Perforations

In this study, three different layouts of perforations are used. The arrangement of perforations is located in the middle of the corrugated web section and along the length of the beam. The first layout (Layout 1) locates the perforations along the corrugated web. It begins from the web near both ends of the TriWP. The second layout (Layout 2) and the third layout (Layout 3) locate the perforations in an alternate arrangement. The alternate arrangement for Layout 2 begins from the first end of the corrugated web of the TriWP. Meanwhile, the alternate arrangement for Layout 3 starting from the second end of the corrugated web of the TriWP. The number of perforations depends on the layout of perforations. Layout 1, Layout 2 and Layout 3 consist of 9, 5 and 4 number of perforations respectively. Fig. 4 to Fig. 6 show examples of the actual views of the respective layout of perforations for circular shape.

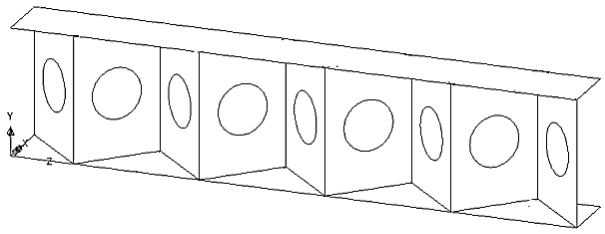

Fig. 4 The isometric view of TriWP with perforation of circular shaped arranged in Layout 1

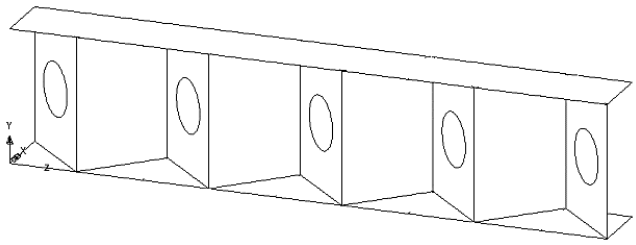

Fig. 5 The isometric view of TriWP with perforation of circular shaped arranged in Layout 2

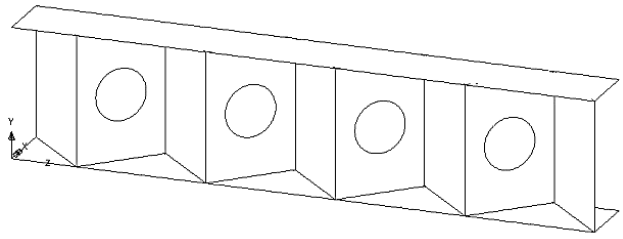

Fig. 6 The isometric view of TriWP with perforation of circular shaped arranged in Layout 3

3. Methodology

There are two stages in this research study; Stage 1 and Stage 2. In Stage 1, the self-weight of TriWP with and without perforation shapes with the dimension of 200 mm × 100 mm × 6 mm × 4 mm and span length of 900 mm is calculated for cases of three different perforation sizes, five different perforation shapes, and three different layouts of perforations. Subsequently, these models have been used in analysis carried out using finite element method to determine the structural efficiency from the ratio of buckling load, P_b to the self-weight under shear loading condition. The increasing load from 0 kN to 120 kN is applied in Stage 1 with the increment of 0 kN, 10 kN, 30 kN, 60 kN, 90 kN and 120 kN. The TriWP with

the most efficient perforation shape, size and layout is selected based on highest structural efficiency determined. In the Stage 2, 10 kN of the load applied as a constant parameter with increasing web thickness and span length are used on selected models in Stage 1 to study the structural behaviour and performance.

3.1 Finite Element Analysis

For this research, all the material properties are adopted from the tensile test with Young's Modulus, E, of 226.53 N/mm^2, shear modulus, G of 79 x 10^3 N/mm^2 and Poisson ratio of 0.3. These material properties remain constant throughout the analysis.

Eigenvalue buckling analysis is used by many researchers such as Valdevit et al. (2006); Moon et al. (2009); Umbarkar et al. (2013); Abidin & Izzudin (2013); Saddek (2015) to obtain critical buckling load by solving the associated eigenvalue problems. The load factors are equivalent to the eigenvalue in an eigenvalue buckling analysis. As mentioned by Abidin & Izzudin (2013), the critical buckling load factor (k_{cr}) for beams under proportional loading may then be determined directly from the eigenvalue solution. Linear eigenvalue buckling analysis will produce critical loads and buckled shapes.

Thin shell element is used in this study. This is because it is more suitable to structural components which the response is mainly due to flexural or in-plane strains, such as the steel plates making up an I-beam. There are two types of thin shell element, such as quadrilateral thin shell element (QSL8) and triangular thin shell element (TSL6). In this study, quadrilateral mesh is used and it will generally give better results than a triangular mesh due to the higher-order variation of forces and moments across the elements.

In shear loading condition, the loading and supports positions as shown in Fig. 7 is adopted from Eldib (2009); Nie et al. (2013); Hamoodi & Gabar (2013). From the Fig., it shows that the condition of the TriWP with perforation after meshing. The symbols of ABCD are presenting the location of the end nodes of TriWP. The nodes for the support are constrained in x, y and z translation direction at one side i.e. AB. Meanwhile, along AC, CD and BD, the supports are constrained in x and z translation. From Eldib (2009); Nie et al. (2013) and Hamoodi & Gabar (2013), the supports are modelled as simply support boundary condition in order to ensure the shear load is applied through the web. On the other hand, the shear loading condition is modelled by applying concentrated load along CD of the vertical stiffener. The concentrated load is applied along one edge of the model to make the web under a pure shear state. Meanwhile, the flanges and stiffeners are replaced with simple support boundary condition for the conservative consideration. However, this study involves the model with and without flanges and their result shows no changes in eigenvalue buckling and buckling modes.

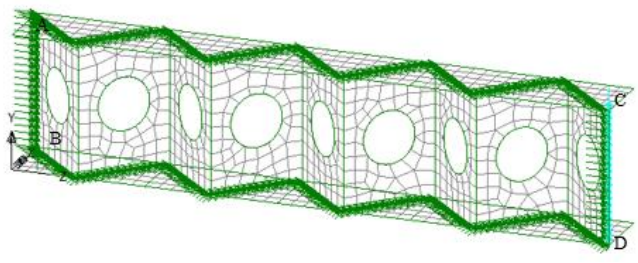

Fig. 7 Supports and loading position of model for shear loading condition

3.2 Determination of Structural Efficiency

The structural efficiency in Stage 1 is calculated based on the ratio of buckling load to the self-weight by using Equation 1. The buckling load is generated from eigenvalue buckling analysis. Higher value of buckling load would produce higher structural efficiency. The comparison between TriWP with and without perforation is made by calculating the percentage difference of structural efficiency by using Equation 2.

$$Efficiency = \frac{Buckling\ load\ (kN)}{self-weight\ (kN)} \quad \text{Eq. 1}$$

$$\%\ of\ structural\ efficiency = \frac{c-d}{c} \times 100 \quad \text{Eq. 2}$$

where;
c = structural efficiency of TriWP without perforation
d = structural efficiency of TriWP with perforation

4. Result

4.1 Percentage weight reduction

The self-weight of TriWP without perforation with the dimension of 200 mm × 100 mm × 6 mm × 4 mm and 900 mm of span length is 0.1616 kN. Table 1 to Table 3 represent the percentage difference of weight reduction of TriWP with and without perforation for Layout 1, Layout 2 and Layout 3, respectively. The presence of perforations such as circular, square, hexagon, octagon and diamond in TriWP reduces the volume of steel usage. Based on the percentage of weight reduction, TriWP with perforation of square shaped shows the highest weight reduction from 0.4D to 0.6D of perforation size for all three layouts of perforations due to the low self-weight compared to another shapes of perforation. The second highest weight reduction is circle which is then followed by hexagon, octagon and diamond. The trend of reduction is significant because it will affect the value of structural efficiency. TriWP with perforation of diamond shaped shows the lowest percentage of weight reduction since it has the highest self-weight. In terms of the layouts of perforations, perforated TriWP with Layout 1 shows the highest percentage of weight reduction ranging from 5.52% to 24.73%. The corresponding percentage values for Layout 2 range from 3.08% to 13.75% and Layout 3 range from 2.47% to 11.01%, respectively. This is because Layout 1 consists of nine numbers of perforations in the web section while Layout 2 and Layout 3 consist of 5 and 4 numbers of perforations, respectively.

Table 1 Percentage difference of weight reduction of TriWP with perforation for Layout 1

Perforation size	Percentage of weight reduction (%)				
	TriWP with perforation shape				
	Circle	Square	Hexagon	Diamond	Octagon
0.4D	8.65	11.01	8.26	5.52	7.85
0.5D	13.50	17.18	12.89	8.61	12.16
0.6D	19.43	24.73	18.55	12.38	17.50

Table 2 Percentage difference of weight reduction of TriWP with perforation for Layout 2

Perforation size	Percentage of weight reduction (%)				
	TriWP with perforation shape				
	Circle	Square	Hexagon	Diamond	Octagon
0.4D	4.82	6.13	4.61	3.08	4.35
0.5D	7.51	9.56	7.18	4.80	6.77
0.6D	10.81	13.75	10.32	6.89	9.74

Table 3 Percentage difference of weight reduction of TriWP with perforation for Layout 3

Perforation size	Percentage of weight reduction (%)				
	TriWP with perforation shape				
	Circle	Square	Hexagon	Diamond	Octagon
0.4D	3.86	4.91	3.69	2.47	3.48
0.5D	6.02	7.66	5.75	3.84	5.42
0.6D	8.65	11.01	8.26	5.52	7.79

4.2 Shear Buckling Capacity

The shear buckling capacity for TriWP without perforation is 39.55 kN. These values come from the shear buckling in the first mode shape. By taking the average of shear buckling capacity, the result of shear buckling capacity for all models is summarized in Table 4. The results of the analysis of TriWP with and without perforation are compared by calculating the percentage difference. The percentage difference is used to present the reduction in shear buckling capacity and it is presented in Table 5. The range of percentage reduction of shear buckling for Layout 1 is 47.9% to 89.05%, 47.9% to 87.69% for Layout 2 and 18.31% to 90.5% for Layout 3. The reduction in shear buckling capacity of TriWP with perforation is found to be more critical when the perforation area increases.

Table 4 Shear buckling capacity of TriWP with perforation

Perforation shape	Shear buckling capacity, kN								
	Layout 1			Layout 2			Layout 3		
	0.4D	0.5D	0.6D	0.4D	0.5D	0.6D	0.4D	0.5D	0.6D
Circle	16.49	11.12	7.44	15.73	10.10	6.79	26.08	16.57	13.16
Square	11.20	7.33	4.33	10.13	11.85	6.37	4.33	3.75	9.64
Hexagon	16.51	11.39	7.99	18.57	9.67	10.26	21.45	15.86	11.89
Diamond	20.58	16.77	13.99	20.58	14.65	11.36	32.27	24.96	16.93
Octagon	14.50	9.46	5.96	13.47	8.29	4.86	20.46	14.34	11.36

Table 5 The percentage difference of shear buckling capacity

Perforation shape	Percentage Difference of Shear Buckling Capacity								
	Layout 1			Layout 2			Layout 3		
	0.4D	0.5D	0.6D	0.4D	0.5D	0.6D	0.4D	0.5D	0.6D
Circle	65.77	71.85	81.15	60.19	74.44	82.82	33.98	58.05	66.68
Square	71.65	81.45	89.05	74.36	70.01	83.87	89.05	90.50	75.59
Hexagon	58.20	71.18	79.78	53.00	75.54	74.03	45.71	59.84	69.89
Diamond	47.90	57.53	64.59	47.90	62.91	71.24	18.31	36.82	57.14
Octagon	63.30	76.06	84.91	65.90	79.02	87.69	48.21	63.69	71.25

Fig. 8 present the shear buckling capacity for all perforation shapes of 0.4D, 0.5D and 0.6D, respectively. It could be observed that the shear buckling capacity for each perforation shape is different. Increasing the perforation area over the web section decreases the shear buckling capacity. It is found that TriWP with perforation of diamond shaped shows the highest shear buckling capacity for Layout 1, Layout 2 and Layout 3 for all three different perforation sizes. However, the perforations are arranged in Layout 3 shows the highest shear buckling capacity due to the reason that the number of perforations in the web section is less than those in Layout 1 and Layout 2. This could be proven that the presence of the perforation in the web section leads to reduction in shear buckling capacity. On the other hand, increasing the perforation size reduces the shear buckling capacity. The percentage of reduction in shear buckling capacity is presented earlier. The lowest reduction in shear buckling capacity recorded is TriWP with perforation of diamond in shape and 0.4D in size arranged in Layout 3 i.e.18.31% (Table 6). That means, the reduction of shear buckling capacity for that model is about 18.31% difference from that of the TriWP without perforation and it shows the lowest drop of shear buckling capacity among other models.

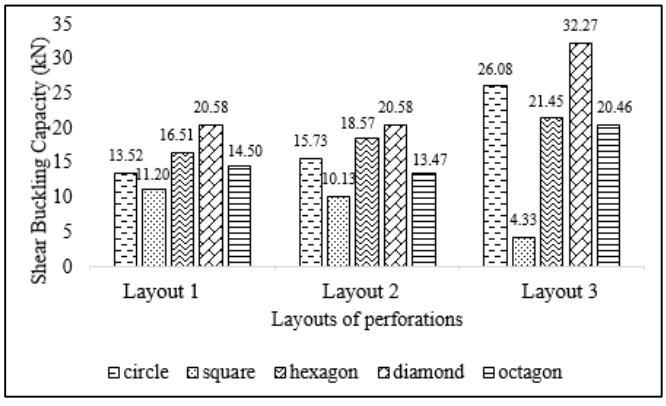

(a)

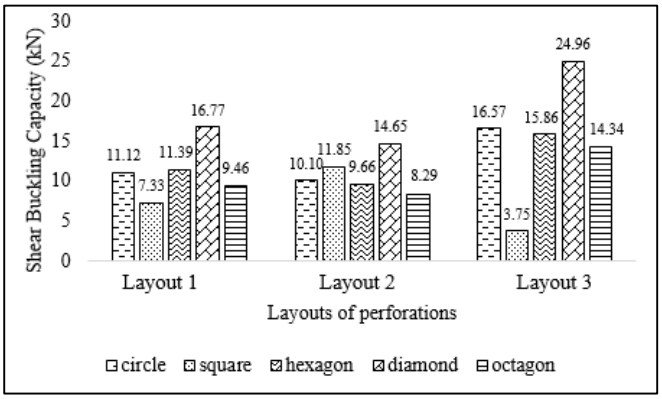

(b)

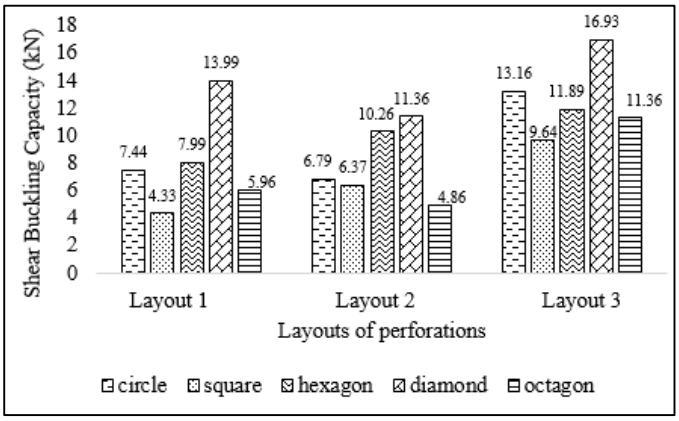

(c)

Fig. 8 Shear buckling capacity of TriWP with perforation of (a) 0.4D, (b) 0.5D and (d) 0.6D

The contribution of this research is to explore the reduction of shear in the corrugated web with triangular web profile. The reduction of the shear buckling capacity is presented in term of percentage difference as shown in Table 6. In this study, it has been proven that TriWP with perforation has lower shear buckling capacity than TriWP without perforation and perforation of diamond shape shows largest shear buckling capacity compared to circle, square, hexagon and octagon.

Table 6 The percentage difference of shear buckling capacity

Perforation shape	Percentage Difference of Shear Buckling Capacity								
	Layout 1			Layout 2			Layout 3		
	0.4D	0.5D	0.6D	0.4D	0.5D	0.6D	0.4D	0.5D	0.6D
Circle	65.77	71.85	81.15	60.19	74.44	82.82	33.98	58.05	66.68
Square	71.65	81.45	89.05	74.36	70.01	83.87	89.05	90.50	75.59
Hexagon	58.20	71.18	79.78	53.00	75.54	74.03	45.71	59.84	69.89
Diamond	47.90	57.53	64.59	47.90	62.91	71.24	18.31	36.82	57.14
Octagon	63.30	76.06	84.91	65.90	79.02	87.69	48.21	63.69	71.25

4.3 Structural Efficiency

The structural efficiency of TriWP with perforation under shear loading condition can be obtained by dividing the shear buckling capacity by the self-weight of the model (refer Eq.1). Table 7 shows the value of structural efficiency of TriWP with perforation. The results show that the value of structural efficiency decreases with increasing perforation size for all perforation shape. The highest value of structural efficiency is found in Layout 3 which is then followed by Layout 2 and Layout 1. In this case, the highest value of structural efficiency of about 204.75 is TriWP with perforation of diamond in shape and 0.4D in size arranged in Layout 3. Meanwhile, the value of structural efficiency for TriWP without perforation is 244.89. The percentage difference of structural efficiency of TriWP with and without perforation is determined and the results are presented in Table 8. On the other hand, TriWP with perforation of diamond in shape and 0.4D in size arranged in Layout 3 is found to be the lowest percentage difference of structural efficiency which is 16.39%. Among the perforation shapes, the highest structural efficiency occurs in the case of diamond shape. This is then followed by circle, hexagon, octagon and square. Therefore, TriWP with perforation of diamond in shape and 0.4D in size arranged in Layout 3 is selected for further analysis in the Stage 2 under shear loading condition.

Table 7 The structural efficiency of TriWP with perforation

Perforation shape	Structural efficiency								
	Layout 1			Layout 2			Layout 3		
	0.4D	0.5D	0.6D	0.4D	0.5D	0.6D	0.4D	0.5D	0.6D
Square	77.87	54.75	35.58	67.13	81.08	45.69	28.15	25.16	67.06
Circle	91.61	79.54	57.17	102.24	67.57	47.10	167.91	109.09	89.17
Hexagon	111.42	80.86	60.70	120.48	64.42	70.80	137.83	104.15	80.24
Diamond	134.78	113.57	98.79	131.41	95.27	75.50	204.75	160.60	110.87
Octagon	97.36	66.64	44.71	87.12	55.01	33.34	131.13	93.87	71.70

Table 8 Percentage difference of structural efficiency

perforation shape	Percentage difference of structural efficiency (%)								
	Layout 1			Layout 2			Layout 3		
	0.4D	0.5D	0.6D	0.4D	0.5D	0.6D	0.4D	0.5D	0.6D
Square	68.20	77.64	85.47	72.59	66.89	81.34	88.50	89.73	72.61
Circle	54.37	67.52	76.65	58.25	72.41	80.77	31.44	55.45	63.59
Hexagon	54.50	66.98	75.21	50.80	73.69	71.09	43.72	57.47	67.23

Diamond	44.96	53.62	59.66	46.34	61.10	69.17	16.39	34.42	54.73
Octagon	60.24	72.79	81.74	64.42	77.53	86.39	46.45	61.67	70.72

Fig. 9 shows the buckling mode for Layout 3 that occurred in the web of TriWP with perforation size of 0.4D for square, circle, hexagon, octagon and diamond perforation and TriWP without perforation. The buckling modes are similar for all perforation shapes. The contour indicates that shear buckling is significant around the perforation shapes. By referring to the literature, such buckling mode is classified as a local shear buckling mode where the buckling involves a single flat panel (Nie et al., 2013).

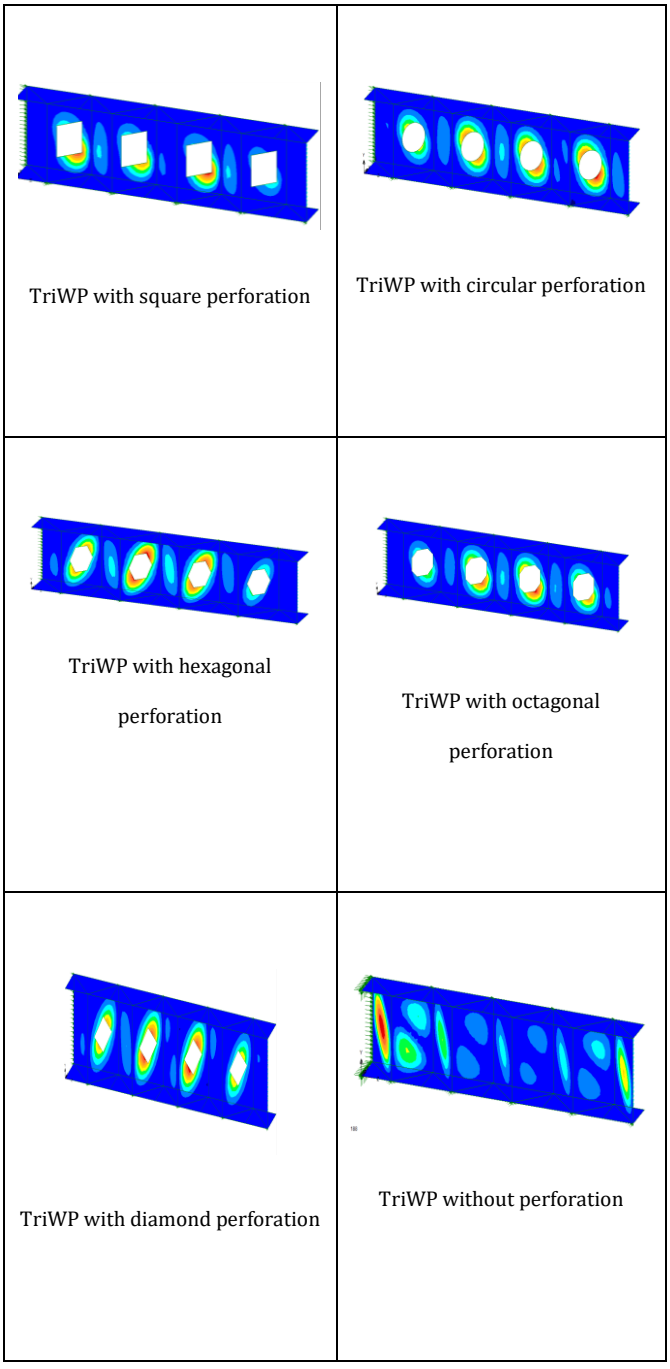

Fig. 9 Result of contour for TriWP with perforation of diamond in shape and 0.4D in size for Mode

4.4 Parametric Study

Section properties have a great effect on the behaviour of beam under shear loading condition. A total of 25 finite element models are analysed under this parametric study to observe the structural behaviour and performance of TriWP with perforation. The model is designed based on the previous stage of numerical analysis where the selected model is chosen based on the structural efficiency i.e. TriWP with perforation of diamond in shape and 0.4D in size arranged in Layout 3. By fixing the depth of the section (D), flange width (B) and the corrugation angle (θ), the models are designed with different web thickness and span length. The constant load applied about 10 kN is used to observe the effect of different section properties.

4.4.1 Effect of Web Thickness, t_w

Each model of TriWP steel section with perforation as shown in Table 9 is designed for different span length from 1 m to 5 m. These 25 models are used to study the influence of web thickness on the structural behaviour under increasing length of the section. Other geometric parameters are kept constant i.e. *D = 200 mm, B = 100 mm, θ = 45° and* t_f *= 8 mm*. The following web thicknesses are considered; t_w *= 2 mm, 4 mm, 5 mm, 6 mm and 7 mm.*

Table 9 Model with different web thickness

Section	Depth, *D* (mm)	Flange width, *B* (mm)	Flange thickness, t_f (mm)	Web thickness, t_w (mm)
200 × 100 × 8 × 2	200	100	8	2
200 × 100 × 8 × 4	200	100	8	4
200 × 100 × 8 × 5	200	100	8	5
200 × 100 × 8 × 6	200	100	8	6
200 × 100 × 8 × 6	200	100	8	7

The results of shear buckling capacity of TriWP with perforation of diamond in shape and 0.4D in size arranged in Layout 3 are presented in Fig. 10. The results show that increasing web thickness from 2 mm to 7 mm has improved the shear buckling capacity. However, the shear buckling capacity is not affected by changing the span length of the model. With the increase in the span length, the shear buckling capacity is found to experience only a slight reduction in shear buckling capacity. At the same span length, the model experienced an increasement in shear buckling capacity when the web thickness increased.

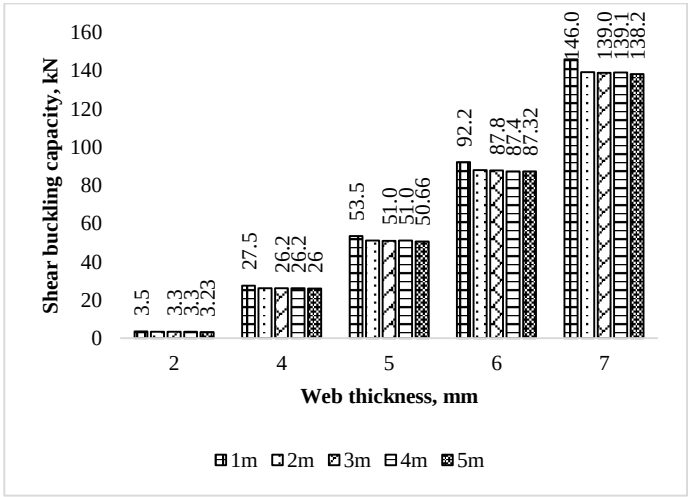

Fig. 10 Shear buckling capacity versus web thickness

According to the theoretical part, the nominal shear strength under pure shear, V_p is given by:

$$V_p = \frac{A_v f_{yw}}{\sqrt{3}} \qquad \text{Eq. 3}$$

That means that the shear buckling capacity is affected by cross-sectional area, specifically the thickness of the web and the overall web depth. In relation to the research, Equation 3 has proven that the shear buckling capacity is not affected by the length of the model. As reported by Tsavdaris and Mello (2012), they noticed that there was no significant reduction in the shear buckling capacity with any beam span. On the other hand, they also prove that there was no effect on thickness of flange on shear buckling capacity where it produces a small effect which could be ignored.

5. Conclusion

Seventy-one models of TriWP with and without perforation have been studied. The self-weight of the models was first determined. They were analysed using finite element analysis to investigate shear deformation. Buckling load were investigated to determine the structural efficiency. The following conclusion can be drawn from the present study:

a) In the first stage of analysis i.e. Stage 1, TriWP with the perforation of diamond in shape and 0.4D in size arranged in Layout 3 showed the highest buckling moment resistance. Therefore, it contributes to the highest value of structural efficiency (204.75) and leads to the most efficient perforation shape, size and layout. Good agreement can be observed between the result of finite element analysis and previous studies found in the literature. Compared to other researchers, the contribution of the analysis of this study is the structural efficiency of TriWP with perforation. The result of analysis is used to determine the structural efficiency of each model.

b) Under shear loading condition, it is found that when the web thickness are increased under the same span length with constant flange and web depth, the value of moment buckling resistance also increased under loading causing shear buckling. Meanwhile, increase in span length of model results in lower shear buckling capacity.

Acknowledgment

The authors would like to express their deepest appreciation to the financial support of Universiti Sains Malaysia (USM under the Research University Grant (RUI) (Account Number: 1001/PAWAM/814222) in funding this project.

References

[1] Driver, R.G., H.H.Abbas, et al., Shear behavior of corrugated web bridge girders. Journal of Structural Engineering, (2006), 132:195.

[2] Seo, J. K., & Mahendran, M., Member moment capacities of mono-symmetric LiteSteel Beam floor joists with web openings. *Journal of Constructional Steel Research*, *70*, (2012), 53–166.

[3] Chung, K. F., Liu, T.C.H. and KO, A.C.H., Investigation on Vierendeel mechanism in steel beams with circular web openings, Journal of Constructional Steel Research, 57(2001), pp.467-490

[4] Tsavdaridis, K. D., & D'Mello, C., Optimisation of novel elliptically-based web opening shapes of perforated steel beams. *Journal of Constructional Steel Research*, *76*, (2012), 39–53.

[5] Tsavdaridis, K. D., & D'Mello, C., Web buckling study of the behaviour and strength of perforated steel beams with different novel web opening shapes. *Journal of Constructional Steel Research*, *67*(10), (2011), 1605–1620.

[6] Darehshouri, S. F., Shanmugam, N. E., & Osman, S., An analytical method for ultimate shear strength of composite plate girders with web openings. *Engineering Structures*, *56*, (2013), 610–620.

[7] Hagen, N. C., Larsen, P. K., & Aalberg, A., Shear capacity of steel plate girders with large web openings, Part I: Modeling and simulations. *Journal of Constructional Steel Research*, *65*(1), (2009), 142–150.

[8] Keerthan, P., & Mahendran, M., Experimental studies of the shear behaviour and strength of lipped channel beams with web openings. *Thin-Walled Structures*, *73*, (2013), 131–144.

[9] Hassanein, M. F., Shear strength of tubular flange plate girders with square web openings. *Engineering Structures*, *58*, (2014), 92–104.

[10] Korani,N.,K., H. R., Lateral bracing of I-girder with corrugated webs under uniform bending. *Journal of Constructional Steel Research*, *66*(12), (2010), 1502–1509.

[11] He, J., Liu, Y., Lin, Z., Chen, A., & Yoda, T., Shear behavior of partially encased composite I-girder with corrugated steel web: Numerical study. *Journal of Constructional Steel Research*, *79*, (2012), 166–182.

[12] He, J., Liu, Y., Chen, A., & Yoda, T., Shear behavior of partially encased composite I-girder with corrugated steel web: Experimental study. *Journal of Constructional Steel Research*, *77*, (2012), 193–209.

[13] Eldib, M. E. a.-H., Shear buckling strength and design of curved corrugated steel webs for bridges. *Journal of Constructional Steel Research*, *65*(12), (2009), 2129–2139.

[14] Nie, J., Zhu, L., Tao, M., & Tang, L., Shear strength of trapezoidal corrugated steel webs. *Journal of Constructional Steel Research*, *85*, (2013), 105–115.

[15] De'nan, F., Effect of Triangular Web Profile on the Shear Behaviour of Steel I-Beam. *Iranica Journal of Energy & Environment*, *4*(3), (2013), 219–222.

[16] Moon, J., Yi, J., Choi, B. H., & Lee, H.-E., Shear strength and design of trapezoidally corrugated steel webs. *Journal of Constructional Steel Research*, *65*(5), (2009),1198–1205.

[17] Chan, R. W. K., Albermani, F., & Kitipornchai, S., Experimental study of perforated yielding shear panel device for passive energy dissipation. *Journal of Constructional Steel Research*, *91*, (2013), 14–25.

[18] Hamoodi, M.J., Gabar, M. S. A., Behavior of Steel Plate Girders with Web Openings Loaded in Shear. *Engineering and Technology Journal*, *31*(15), (2013), 2982–2996.

[19] Yan. K. J., & F. D., *Numerical study on Shear Behaviour for Triangular Steel Section with opening*. Universiti Sains Malaysia, (2012).

[20] Yi, J., Gil, H., Youm, K., & Lee, H., Interactive shear buckling behavior of trapezoidally corrugated steel webs. *Engineering Structures*, *30*(6), (2008), 1659–1666.

[21] British Standard 5950-1:2000. Structural use of steelwork in building. Part 1, Code of practice for design-rolled and welded sections

[22] Saddek, A. B. (2015). Theoretical Investigation of Shear Buckling for Hybrid Steel Plate Girder with Corrugated Webs. *World Applied Sciences Journal*, 2, p. 284-302